c-Met-Mediated Reactivation of PI3K/AKT Signaling Contributes to Insensitivity of BRAF(V600E) Mutant Thyroid Cancer to BRAF Inhibition

Hyung Kwon Byeon,[1] Hwi Jung Na,[1] Yeon Ju Yang,[1] Hyeong Ju Kwon,[2] Jae Won Chang,[3] Myung Jin Ban,[4] Won Shik Kim,[1] Dong Yeob Shin,[5] Eun Jig Lee,[5] Yoon Woo Koh,[1]* Joo-Heon Yoon,[1,6,7] and Eun Chang Choi[1]

[1]*Department of Otorhinolaryngology, Yonsei University College of Medicine, Seoul, Republic of Korea*
[2]*Department of Pathology, Yonsei University College of Medicine, Seoul, Republic of Korea*
[3]*Department of Otorhinolaryngology, Chungnam National University College of Medicine, Daejeon, Republic of Korea*
[4]*Department of Otorhinolaryngology, Soonchunhyang University College of Medicine, Cheonan, Republic of Korea*
[5]*Department of Internal Medicine, Yonsei University College of Medicine, Seoul, Republic of Korea*
[6]*The Airway Mucus Institute, Yonsei University College of Medicine, Seoul, Republic of Korea*
[7]*Research Center for Human Natural Defense System, Yonsei University College of Medicine, Seoul, Republic of Korea*

BRAF (V600E) mutation is the most commonly detected genetic alteration in thyroid cancer. Unlike its high treatment response to selective BRAF inhibitor (PLX4032) in metastatic melanoma, the treatment response in thyroid cancer is reported to be low. The purpose of this study is to investigate the resistance mechanism responsible for this low treatment response to BRAF inhibitor in order to maximize the effect of targeted therapy. We examined the expression of feedback regulation mechanisms and alterations in the upper signal transduction pathway in thyroid cancer cell lines harboring BRAF mutation. Also, we investigated the effect of dual inhibition from combinatorial therapy. Two thyroid cancer cell lines, 8505C (anaplastic thyroid cancer) and BCPAP (papillary thyroid cancer) were selected and treated with PLX4032 and its drug sensitivity were examined and compared. Further investigation on the changes in signals responsible for the different treatment response to PLX4032 was carried out and the same experiment was performed on orthotopic xenograft mouse models. Unlike BCPAP cells, 8505C cells presented drug resistance to PLX4032 treatment and this was mainly due to increased expression of c-Met. Effective inhibitions of c-Met, p-AKT, and p-ERK were achieved after dual treatment with BRAF inhibitor (PLX4032) and c-Met inhibitor (PHA665752). Similar results were confirmed by in vivo study with orthotopic xenograft mouse model. c-Met-mediated reactivation of the PI3K/AKT pathway and MAPK pathway contributes to the relative insensitivity of BRAF (V600E) mutant anaplastic thyroid cancer cells to PLX4032. Dual inhibition of BRAF and c-Met leads to sustained treatment response.

Key words: thyroid neoplasm/drug therapy; molecular targeted therapy; drug resistance; mutation

INTRODUCTION

Thyroid cancer is the most common malignancy of the endocrine system with preponderance shown in women. Histologically, carcinoma comprises approximately 98% of all thyroid malignancies. Papillary carcinoma is the most common thyroid carcinoma (80%), followed by follicular carcinoma (10–15%), medullary carcinoma (5–10%), and anaplastic carcinoma (2–5%) [1–4]. Surgery, postoperative radioactive iodine therapy, and TSH suppression by L-thyroxine administration form the basis of the treatment of well differentiated thyroid cancers. Treatment results can be disappointing in some advanced stage cancers, despite aggressive managements including conventional chemotherapy and radiotherapy. Anaplastic carcinoma in particular, has a very poor prognosis since it is highly invasive and presents extensive locoregional invasion or systemic progression at initial diagnosis [5].

Multiple genetic alterations or mutations are involved in the tumorigenesis of thyroid cancer [6].

Abbreviations: Annexin V-FITC/PI, annexin V-fluorescein isothiocyanate/propidium iodide; BSA, bovine serum albumin; DAPI, 4'6-diamidino-2-phenylindole; DMSO, dimethyl sulfoxide; EGFR, epidermal growth factor receptor; ERK, extracellular single-regulated kinase; FACS, fluorescence-activated cell sorting; FBS, fetal bovine serum; HGF, hepatocyte growth factor; IGF1R, insulin-like growth factor 1 receptor; MAPK, mitogen-activated protein kinase; MEK, mitogen-activated protein/extracellular signal-regulated kinase; MMP, mitochondrial membrane potential; MTT, 3-(4,5-dimethylthiazol-2-yl)-2,5-diphenyl-tetrazolium bromide; OD, optical density; PBS, phosphate buffered saline; PFA, paraformaldehyde; PMSF, phenylmethylsulfonyl fluoride; RTK, receptor tyrosine kinases; SDS-PAGE, sodium dodesyl sulfate-polyacrylamide gel electrophoresis; TBS, tris buffered saline; TSH, thyroid-stimulating hormone; TUNEL, terminal deoxynucleotidyl transferase (TdT)-mediated dUTP-biotin nick end labeling.

Grant sponsor: National Research Foundation of Korea; Grant number: 2010-0012412; Grant sponsor: Yonsei University College of Medicine Research; Grant number: 6-2014-0052

*Correspondence to: Department of Otorhinolaryngology, Yonsei University College of Medicine, Severance Hospital, Yonsei University Health System, 50 Yonsei-ro, Seodaemun-gu, Seoul 120-752, Republic of Korea.

Received 27 February 2015; Revised 26 July 2015; Accepted 18 September 2015

DOI 10.1002/mc.22418

Published online 12 October 2015 in Wiley Online Library (wileyonlinelibrary.com).

Thyroid somatic mutations include the MAPK signal transduction pathway. RET tyrosine kinase of the cell membrane from mutated genes activates the MAPK pathway and up-regulates intracellular transducers RAS and B type RAF (BRAF), which in turn activates MEK and ERK, thereby resulting in intranuclear signal transduction for cellular proliferation, differentiation, and survival. The most heavily studied and commonly found genetic alteration in thyroid cancer is the BRAF mutation. BRAF is a serine-threonine kinase which is activated and bound by RAS and then translocated to the cell membrane. The most commonly identified BRAF mutation in thyroid cancer is the substitution of valine to glutamic acid at residue 600 (V600E) caused by the point mutation of nucleotide position 1799. BRAF (V600E) mutation is most common in papillary carcinomas however, it is found in a third of undifferentiated or anaplastic carcinomas. BRAF mutation causes constitutive BRAF kinase activity and sustained activation of MAPK cascade through phosphorylation of MEK and ERK kinase. BRAF mutation is closely related to aggressive clinical and pathologic features of thyroid cancer such as lymphatic metastases, extrathyroidal capsular invasion, advanced clinical stage, tumor recurrence, reoperation, and cancer-related deaths.

Besides thyroid cancer, BRAF (V600E) mutation is also detected in approximately 50% of malignant melanoma, 15% of colorectal cancer, and nearly all cases of hairy-cell leukemia [7–9]. PLX4032 (vemurafenib), a selective BRAF inhibitor has been recently approved by the FDA for the treatment of BRAF (V600E) mutant metastatic melanoma, which has shown to improve progression-free survival and overall survival in 80% of patients. Improved treatment response was also noted in hairy-cell leukemia [10,11]. Despite its high treatment response in malignant melanoma, its effects are insignificant in other solid tumors harboring BRAF mutation. The therapeutic effect of PLX4032 in patients with BRAF mutant colorectal cancer is merely 5%, and the effect of selumetinib, a MEK inhibitor, in thyroid cancer has no effect, contrary to expectations [12,13]. This discrepancy in treatment response comes from the manifestation of resistance mechanisms against targeted therapeutic agents [14]. Regarding the fact that thyroid cancer also shows therapeutic resistance to BRAF inhibition as in colorectal cancer, the aim of the present study is to elucidate the resistance mechanism which has not been extensively investigated to date in order to maximize the effect of targeted therapy. We examined the expression of feedback regulation mechanisms and alterations in the upper signal transduction pathway in various thyroid cancer cell lines harboring BRAF mutation. Also we investigated the effect of dual inhibition from combinatorial therapy.

MATERIALS AND METHODS

Cell Culture

BRAF (V600E) mutant thyroid cancer cell lines, 8505C (anaplastic thyroid cancer), and BCPAP (papillary thyroid cancer) were maintained in 10% RPMI medium at 37°C with 5% CO_2 under humidified conditions.

Cell Proliferation Assay

Thyroid cells (8505C, BCPAP) were seeded in 96-cell well plates at a density of 1×10^3 cells per well and were incubated for 24 h at 37°C with 5% CO_2. For each sample, it was treated with PLX4032 of varying concentrations and was incubated for 24 and 48 h. Two microgram per milliliter of MTT test solution (Sigma–Aldrich, St. Louis, MO) were added to each well and after 4 h of incubation, 100 μg DMSO was added for each well and OD was measured at 570 nm.

FACScan With Annexin V-FITC/PI Staining

3×10^5 cells were seeded onto 6-well culture dishes and cultured and after 24 h of starvation, the cells were treated with 1 μM PLX4032 and cultured with time variation. Culture fluid was removed and the cells were washed three times with PBS, transferred in 1.5 ml tubes, and resuspended in Annexin V-FITC Apoptosis Detection kit I (Bio-vision, San Francisco, CA) binding buffer and Annexin V-FITC. After 5 min reaction at room temperature, apoptosis was detected using BD FACSVerse (Flow cytometer).

TUNEL Assay

Cells were fixed in 1% PFA containing PBS (pH 7.4) at room temperature for 10 min, and after washing, the cells were incubated with 5 μl TUNEL enzyme (Roche Molecular Biochemicals, Basel, Switzerland) and 45 μl TUNEL label (Roche Molecular Biochemicals) mixture for 1 h at 37°C. The stained cells were then visualized with confocal microscopy (Carl Zeiss, Oberkochen, Germany) at 515–565 nm.

Pathscan RTK Signaling Antibody Array

An antibody array for simultaneous detection of RTK and key signaling nodes was used (Cell signaling technology Inc., Danvers, MA). All target RTKs or kinases were detected with a phospho-specific or a pan-tyrosine recognizing antibody as indicated in the manual of the array. 8505C cells were treated with DMSO or PLX4032 for 9 h. The cells were then harvested and cell lysates were prepared according to the manufacturer's instructions and hybridized to the slides containing pre-spotted target-specific antibodies. Detection was done using a biotin-streptavidin-conjugated antibody with an image analysis software. Relative levels of phosphorylated RTK or other signaling proteins in DMSO-treated cells compared to PLX4032-treated cells were calculated from three independent experiments.

Confirmation of c-Met Expression and c-Met Inhibitor-Induced Suppression of c-Met Expression by Western Blot Analysis

Thyroid cell lines were washed with PBS and were treated with lysis buffer (10 mM Tris-HCl (pH 7.4), 100 mM NaCl, 1 mM EDTA, 1 mM EGTA, 1 mM NaF, 20 mM $Na_4P_2O_7$, 2 mM Na_3VO_4, 1% Triton X-100, 10% glycerol, 0.1% SDS, 0.5% deoxylcholate) (Invitrogen, Camarillo, CA), 1 mM PMSF and protease inhibitors cocktail (Sigma–Aldrich) and then harvested. The protein was centrifuged under 13,200 rpm for 10 min and the supernatant was used for Western blot analysis where the protein amount was quantified with Pierce BCA Protein Assay Kit (Thermo, Rockford, IL). The lysates were subjected to 10% SDS-PAGE to separate proteins. An equal amount of protein (30 μg) was loaded per well and the proteins were transferred onto p-c-Met (1:1,000), p-AKT (1:1,000), p-ERK(1:1,000), GAPDH (1:1,000) to be left at 4°C overnight incubation. The next day, it was thoroughly washed with TBS containing 0.1% Tween-20, and then reacted with secondary rabbit antibody (Jackson, West Grove, PA) and anti-mouse antibody (Jackson) to be visualized on X-ray film using SuperSignal West Pico Chemiluminescent Substrate (Thermo).

Transient Transfection of c-Met and RNA Interference (siRNA)

2×10^5 cells per well were seeded onto 6-well culture dishes containing 2 ml antibiotic-free medium supplemented with 10% FBS. The cells were incubated at 37°C with 5% CO_2 until the cell monolayers achieved 60–80% confluence. Next, 500 μl optimum and 10 μl RNAiMAX, and 500 μl optimum and 5 μl RNAi were mixed and left at room temperature for 5 min, and then mixed together. After 20 min, droplets of the mixture were applied at the cells and left to react for 6 h. Thereafter, the medium was changed to 10% FBS and penicillin-steptomycin supplemented medium and the cells were incubated at 37°C with 5% CO_2 for 48 h. Subsequently, PLX4032 was treated for 6 h and the cells were harvested and confirmed by Western blot analysis.

HGF ELISA

The media was gathered and concentrated before Western blot analysis. Quantikine ELISA human HGF (R&D Systems co., Minneapolis, MN) was used on concentrated media. One hundred and fifty microliters Assay diluent RD1W was applied to 50 μl media and incubated for 2 h. Then it was washed four times with 400 μl wash buffer solution and was incubated for 1.75 h after treatment of 200 μl HGF conjugate. It was then washed four times again with the wash buffer and after dimming the light, 50 μl substrate solution was added and incubated for 30 min, followed by treatment of 50 μl stop solution for measurement of OD at 450 nm.

Orthotopic Xenograft Mouse Model

8505C cells were harvested and 1×10^5 cells suspended in 5 μl PBS were injected orthotopically in the right thyroid gland of male athymic nude BALB/c mice, aged 6 wk (Orientbio Inc., Seongnam-si, Korea) using a 25 μl Hamilton syringe (Hamilton Company, Reno, NV). Tumor formation was confirmed at 3 wk post-injection, and the mice were randomly divided into four groups of four. The control group was treated with DMSO and the other three groups were each injected with PLX4032, PHA665752, PLX4032, and PHA665752 combination respectively, three times a week for 3 wk. The animals were then euthanized and Western blot analysis, H&E staining, and immunohistochemical analysis were carried out from tissue samples. All procedures of the animal experiment were approved by the Committee for ethics in animal experiments of Yonsei University College of Medicine and all animals in the experiment were handled in accordance with the Guide for the care and use of laboratory animals in Department of laboratory animal resources, Yonsei University College of Medicine.

Immunohistochemical Analysis

The tumor tissue samples from mice were processed for paraffin section and were undergone deparaffinization consequently with xylene and ethanol. Antigen retrieval was done for 15 min followed by reaction with H_2O_2 for 10 min and blocking (10% normal goat serum + 0.01% BSA + dilution) for 1 h. The slides were then incubated overnight at 4°C with primary anti-c-Met and AKT antibody (1:200). Next, the slides were treated with secondary anti-rabbit antibodies (1:500) for 1 h and reacted using DAB histochemistry kit (Life technologies, Rockford, IL). Finally the slides were stained with hematoxylin and processed with mounting solution (DAKO) and visualized using a microscope.

Statistical Analysis

All the data were derived from three independent experiments, and the parameters were expressed as the means ± SD. "Student's" t test and one way ANOVA were performed using SPSS 20.0 statistical software (SPSS, Chicago, IL). A $P < 0.05$ was considered statistically significant (* $P < 0.05$; ** $P < 0.01$; *** $P < 0.001$).

RESULTS

PLX4032 Shows Different Drug Sensitivity Against Different BRAF (V600E) Mutant Thyroid Cancer Cell Lines

To evaluate the drug sensitivity of BRAF inhibitor, PLX4032 on BRAF mutant thyroid cancer, two different BRAF (V600E) mutant thyroid cancer cell lines, 8505C and BCPAP were used. Cell lines were treated with PLX4032 for 24 h and cell viability was analyzed by MTT assay. The results revealed that 8505C cells showed some degree of proliferation

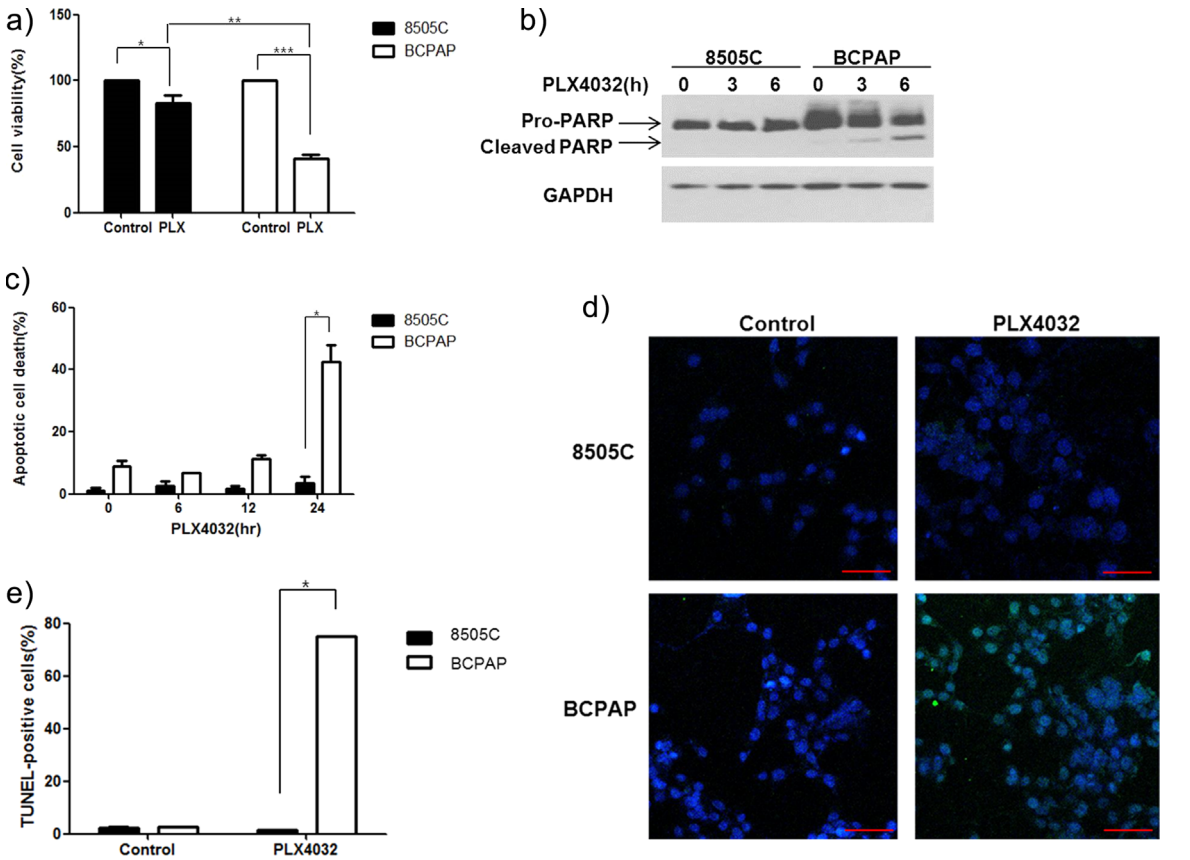

Figure 1. Differential drug sensitivity of BRAF (V600E) mutant thyroid cancer cell lines 8505C and BCPAP to PLX4032 treatment. (a) MTT assay done after treatment with 3 μM PLX4032 for 24 h showed that the cell viability was higher in 8505C. (*$P < 0.05$, **$P < 0.01$, ***$P < 0.001$) (b) Western blot analysis after treatment with 1 μM PLX4032 of increasing treatment times. PLX4032-induced cleaved PARP expression was more prominent in BCPAP cells as compared to the 8505C cells. (c) Analysis of apoptotic cell death with Annexin V-FITC/PI staining. 1 μM PLX4032 was treated for 6, 12, and 24 h to both 8505C and BCPAP cells. Apoptosis was substantially increased in BCPAP cells. (*$P < 0.05$) (d) TUNEL assay. Cells were treated with 1 μM PLX4032 for 6 h. PLX4032-induced TUNEL-positive cells were more prominently increased in BCPAP cells compared to 8505C cells. (e) Quantification of apoptotic cells from TUNEL assay. TUNEL-positive cells were significantly increased in BCPAP cells after PLX4032 treatment. (*$P < 0.05$).

despite drug treatment, however BCPAP cells presented approximately 40% apoptosis (Figure 1a).

To determine whether the PLX4032-induced cell death was due to apoptosis, several assays of apoptosis were performed. Unlike BCPAP cells, 8505C cells showed constant and unaffected survival following PLX4032 treatment (Figure 1b). From the FACS using Annexin V-FITC/PI staining, PLX4032-induced cell apoptosis was less prominent in 8505C cells as compared to BCPAP cells (Figure 1c). Similar results were observed from TUNEL assay (Figure 1d,e).

PLX4032 Induces Over-Expression of p-c-Met and Subsequently Over-Expression of PI3K/AKT Pathway in 8505C

When 8505C cells were treated with PLX4032 and cell viability assessed until 2 d, it was unaffected, moreover increased with respect to control (Figure 2a). According to RTK array after PLX4032 treatment, specific over-expression of c-Met was confirmed (Figure 2b). Analysis of p-c-Met expression in the 8505C and BCPAP cells by Western blot analysis revealed that p-c-Met expression was significantly increased in 8505C cells according to increased treatment times of PLX4032 whereas it was unchanged in BCPAP cells (Figure 2c).

To investigate the PLX4032-induced over-expression of p-c-Met, the BRAF inhibitor was treated to 8505C cells at different levels of concentrations and treatment times. Expressions of p-c-Met were constantly increased according to treatment of increased concentrations of PLX4032 and subsequently p-AKT expressions were also increased (Figure 3a). Similar patterns were also noted according to increased drug treatment times where p-c-Met sequentially increased until 9 h (Figure 3b). The therapeutic effect of PLX4032 in 8505C cells could be verified by the decreased expression of p-ERK. However p-ERK levels showed mild rebound increase after 9 h treatment of PLX4032. Expression levels of p-AKT were increased following the increased expression of p-c-Met. When c-Met was knocked down and PLX4032 treated with increasing times,

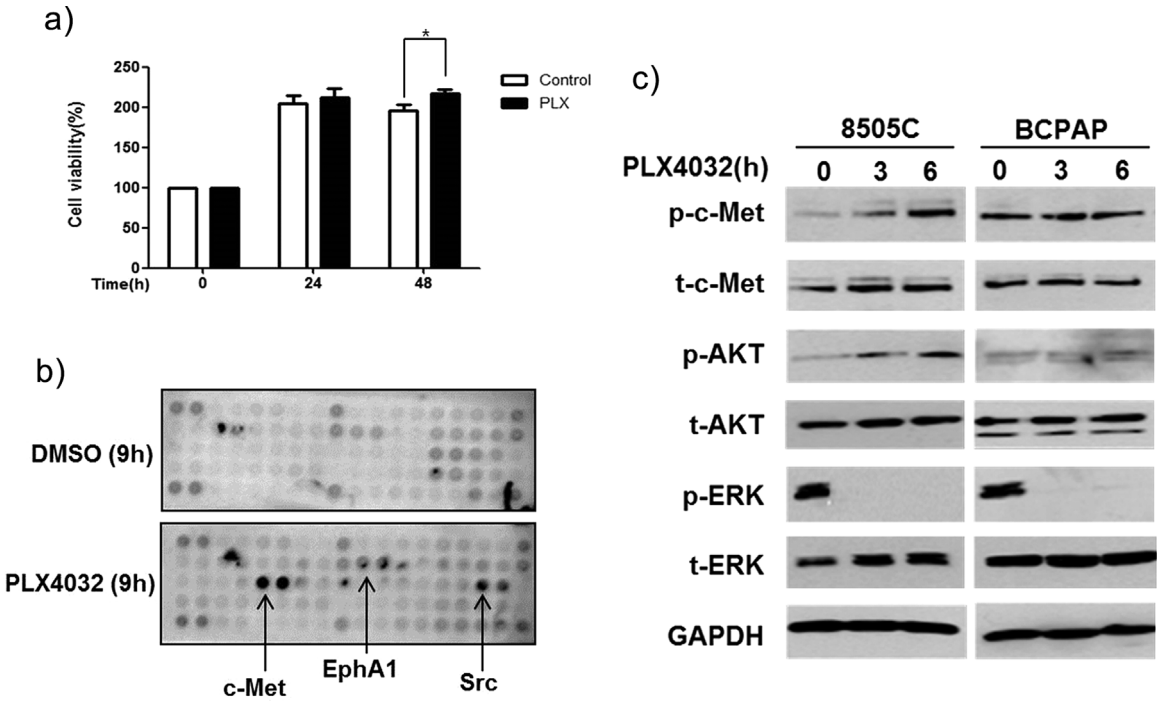

Figure 2. Resistance from PLX4032 is related to over-expression of p-c-Met in 8505C. (a) MTT assay done after treatment with 3 μM PLX4032 until 48 h in 8505C cells. Cell proliferation was unaffected by PLX4032 treatment. (*$P < 0.05$) (b) RTK array after treatment with 3 μM PLX4032 for 9 h in 8505C cells. c-Met expression was specifically detected. (c) Western blot analysis after treatment of 1 μM PLX4032 for 3 and 6 h in both 8505C and BCPAP cells. Unlike BCPAP cells, p-c-Met expression was increased through increased treatment times of PLX4032 in 8505C cells.

both c-Met and p-AKT expression levels were decreased (Figure 3c).

Inhibition of c-Met can Reverse the Over-Expression of PI3K/AKT Pathway After Treatment of PLX4032 in 8505C

Following the combinatorial treatment of PLX4032 with PHA665752, a c-Met inhibitor, p-c-Met levels were not increased and p-AKT expression level was relatively low (Figure 4a). Following single treatment of PHA665752, p-c-Met expression levels were decreased however p-AKT and p-ERK levels were unchanged (Figure 4b). From the MTT and TUNEL assay (Figure 4c,d), drug-induced cell apoptosis was more prominent following combinatorial treatment of PLX4032 and PHA665752 than single agent treatment, and same results were confirmed from Western blot analysis of PARP expression (Figure 4e).

PLX4032 Induces the Expression of HGF in 8505C

HGF ELISA was done in 8505C and BCPAP cells after PLX4032 treatment and the results demonstrated that levels of HGF, the c-Met ligand were increased in 8505C cells but unchanged in BCPAP cells (Figure 5a). The increased HGF expression level in 8505C from PLX4032 treatment was mainly noted in the media (Figure 5b). Western blot analysis was done after treatment of PLX4032, PHA665752, and HGF (Figure 5c). Expression of p-c-Met was increased following PLX4032 treatment, more increased after HGF treatment, and most increased following treatment of both. Similar results were also noted for p-AKT. After dual treatment of PLX4032 and PHA665752, expression levels of p-c-Met, p-AKT, and p-ERK were all decreased.

Combinatorial Treatment of PLX4032 and PHA665752 can Inhibit the Tumor Growth in an Orthotopic Xenograft Mouse Model

The in vitro results were verified also in vivo. The tumor size was similar or slightly larger in the PLX4032 and PHA665752 single treatment group with reference to the control group, however, the tumor size was significantly smaller in the combinatorial treatment group (Figure 6a). From the assessment of tumor volume and weight, the values were larger in the mice of PLX4032 single treatment group compared to the DMSO treated mice, however, both values were significantly lower in the mice with combinatorial treatment of PLX4032 and PHA665752 (Figure 6b). From the analysis of protein expression levels in tumor specimens, p-c-Met expression was increased in PLX4032 single treatment group however it was considerably decreased in combinatorial drug treatment group (Figure 6c). Levels of p-AKT expression were also high in PLX4032 single treatment group and significantly low in combinatorial treatment group. Histopathological analysis was performed by hematoxylin and eosin (H & E) staining from tumor specimens

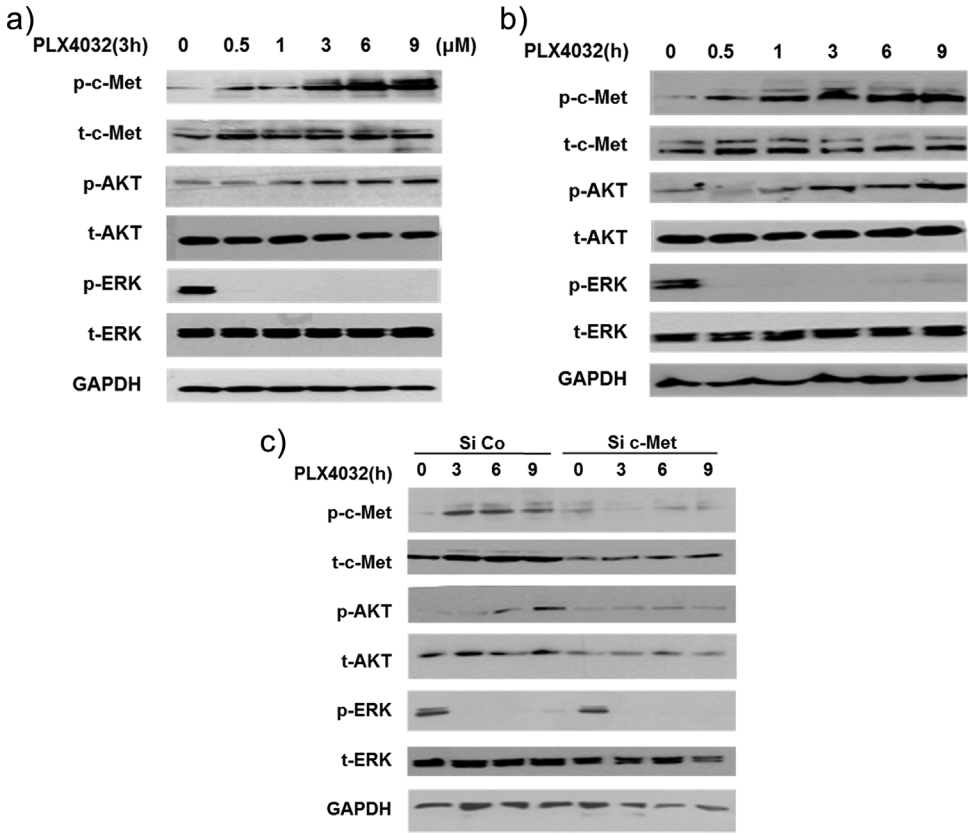

Figure 3. PLX4032 treatment induces over-expression of p-c-Met and subsequently over-expression of PI3K/AKT pathway in 8505C. (a) Western blot analysis after treatment of PLX4032 of increasing dosages for 3 h in 8505C cells. p-c-Met expression levels were increased and p-AKT levels were subsequently increased according to increased dosages of PLX4032 treatment. (b) Western blot analysis after treatment of 1 μM PLX4032 of increasing treatment times in 8505C cells. p-c-Met expression levels were increased and p-AKT levels were subsequently increased according to increased treatment times of PLX4032. (c) 8505C cells transfected with c-Met small interfering RNA (siRNA) or negative control siRNA were treated with 1 μM PLX4032 for 3, 6, and 9 h. Following knockdown of c-Met, p-c-Met and p-AKT expression levels were constantly decreased.

of mice from each treatment group (Figure 6d). The tumors from drug-treatment groups generally presented tumor capsule formation with pushing margins whereas the tumor of the control group showed irregular infiltrative growth with no evidence of tumor capsule. More specifically, the PLX4032 single treatment group showed further aggressive features such as frequent extracapsular extension, lymphovascular invasion, and perineural invasion. The combinatorial drug treatment group however presented no tumor capsule invasion with lymphocytes aggregating around the tumor and absence of lymphovascular invasion and perineural invasion. Cellular change of degeneration and decreased cell viability was noted in all drug-treatment groups when compared to highly viable tumor cells of the control group, but the degree was most prominent in the combinatorial treatment group. Furthermore, immunohistochemistry to demonstrate intratumoral protein expression levels in tumor tissues of each treatment groups confirmed high detection levels of p-c-Met and p-AKT in the PLX4032 single treatment group. Both levels were markedly decreased in the combinatorial drug treatment group however, with low detection of p-ERK (Figure 6e).

DISCUSSION

Anaplastic thyroid cancer which comprises approximately 5% of all thyroid carcinomas is considered highly aggressive and presents an extremely poor prognosis since it is resistant to conventional treatment modalities. In addition, conventional chemotherapy and radiation frequently cause serious post-treatment complications such as extensive tissue fibrosis, wound cicatrization, and edema and it can lead to eventual deterioration of patients' quality of life due to varying degrees of swallowing and voice problems. Therefore it is imperative for development of tumor-specific targeted agents with relatively low toxicity.

The BRAF kinase is the most potent activator of the MAPK signal cascade which is involved in cellular growth, differentiation, and carcinogenesis. BRAF (V600E) mutation is present in 29–70% of papillary thyroid cancer [15–18], approximately 26% of anaplastic

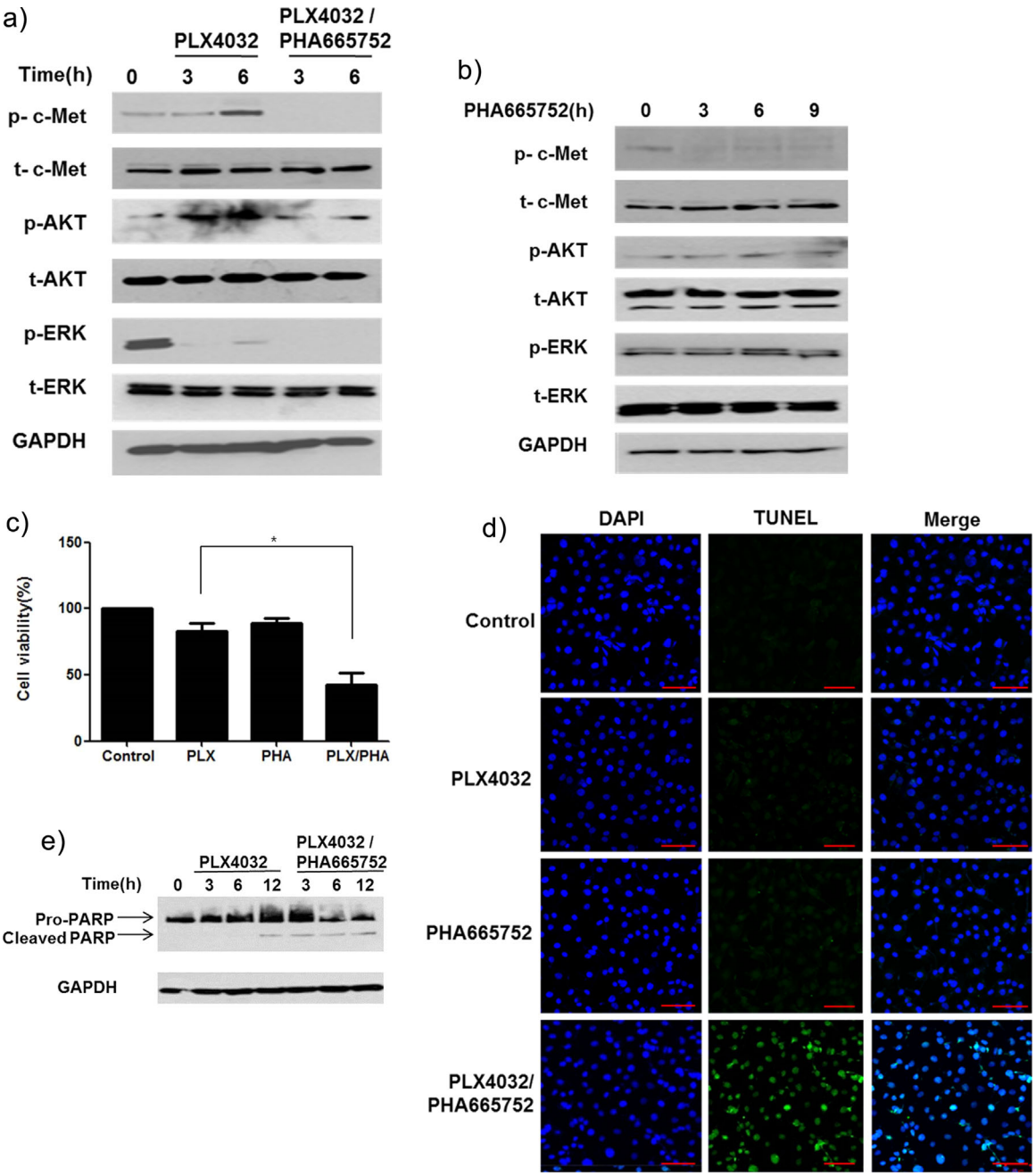

Figure 4. Combinatorial treatment of PLX4032 and PHA665752 has maximal therapeutic efficacy in 8505C tumor cells. (a) Western blot analysis of each after treatment of 1 μM PLX4032 and dual treatment of 1 μM PLX4032 and 0.5 μM PHA665752 for 3 and 6 h in 8505C cells. The increased levels of p-c-Met and p-AKT expression after PLX4032 treatment were suppressed together with p-ERK suppression by combinatorial treatment of PLX4032 and PHA665752. (b) Western blot analysis after treatment of 0.5 μM PHA665752 for 3, 6, and 9 h in 8505C cells. p-c-Met expression levels were decreased, however, p-AKT and p-ERK levels were unaffected. (c) MTT assay done after different drug treatment conditions for 24 h in 8505C cells. Cell proliferation was significantly decreased after dual treatment of 1 μM PLX4032 and 0.5 μM PHA665752. ($^*P < 0.05$) (d) TUNEL assay. 8505C cells were each treated under different drug regimens. TUNEL-positive cells were most prominently increased after combinatorial treatment of 1 μM PLX4032 and 0.5 μM PHA665752 for 6 h. (e) Western blot analysis of each after treatment of 1 μM PLX4032 and dual treatment of 1 μM PLX4032 and 0.5 μM PHA665752 in 8505C cells. Drug-induced cleaved PARP expression was more prominent following combinatorial treatment of PLX4032 and PHA665752.

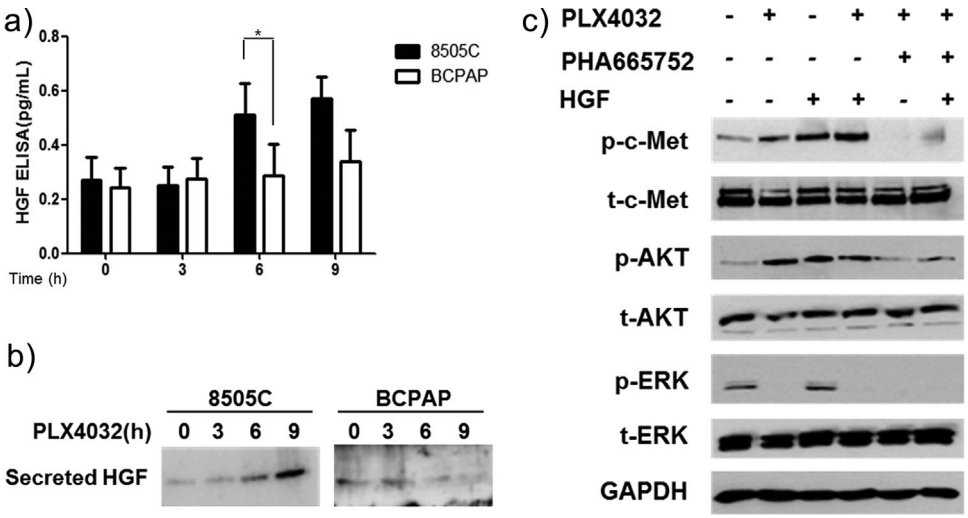

Figure 5. PLX4032 induces the expression of HGF in 8505C. (a) HGF ELISA after 1 μM PLX4032 treatment of increasing duration in 8505C and BCPAP cells. HGF levels were significantly increased in 8505C cells. (*$P < 0.05$) (b) Western blot analysis after treatment of 1 μM PLX4032 for 3, 6, and 9 h in 8505C and BCPAP cells. HGF expression levels within the media (secreted HGF) were increased in 8505C cells. (c) Western blot analysis after different treatment conditions consisting of 1 μM PLX4032, 0.5 μM PHA665752, and 30 ng/ml HGF for 9 h in 8505C cells. p-c-Met expression was increased together with p-AKT expression after PLX4032 and HGF treatment but were effectively suppressed after combinatorial treatment of PLX4032 and PHA665752.

thyroid cancer [19], and other malignancies such as colorectal cancer, ovarian cancer, lung cancer, and hepatobiliary cancer [9]. Unlike the high treatment response of PLX4032 in BRAF (V600E) mutant melanoma, the selective BRAF inhibitor was not as effective in other BRAF (V600E) mutant solid tumors. According to Corcoran et al., when PLX4032 was treated to BRAF mutant colorectal cancer, p-ERK signal was transiently suppressed, however, it was soon re-activated due to EGFR-mediated RAS and CRAF activation [14,20]. Therefore when both BRAF and EGFR signals were suppressed, the MAPK signal pathway could be effectively suppressed thereby improving the therapeutic efficacy. Straussman et al. discovered that stromal secretion of HGF contributes to innate resistance to BRAF inhibition in drug resistant BRAF (V600E) mutant melanomas [21]. Montero-Conde et al. showed that only transient suppression of ERK signal was achieved following BRAF and MEK inhibition in BRAF (V600E) mutant thyroid cancer, and this rebound phenomenon was the result of HER3 signal elevation [22]. In this process, neuregulin-1 (NRG1), a HER3 ligand, was also induced by PLX4032. In this context, we investigated in detail the resistance mechanism against BRAF inhibition in BRAF (V600E) mutant thyroid cancer which has not been extensively studied, to provide an effective targeted therapy.

In the present study, changes in the signaling pathway following PLX4032 treatment in two different thyroid cancer cell lines, 8505C and BCPAP, harboring BRAF (V600E) mutation were investigated. Interestingly, contrary responses were discovered between 8505C and BCPAP. Favorable treatment responses were shown in BCPAP cells, however resistance against PLX4032 was demonstrated in 8505C cells (Figure 1). The causative mechanism for this different drug sensitivity in different types of BRAF (V600E) mutant thyroid cancer is unknown and is beyond the scope of this study but further investigation would be needed. On the basis of these findings, when 8505C cells were treated with the selective BRAF inhibitor, it could be inferred that a specific drug resistance mechanism was responsible for this decreased treatment response, and to further elucidate this resistance mechanism, alterations in signaling following PLX4032 treatment of varying drug concentrations and treatment times in 8505C cells were investigated. The results showed that expression levels of p-c-Met were specifically increased and p-AKT levels were consecutively increased (Figure 2,3). These results suggest that BRAF inhibition in 8505C cells leads to over-expression of c-Met which in turn results in re-activation of MAPK pathway and also PI3K/AKT pathway. The rebound phenomenon of the p-ERK signal from PLX4032 treatment could be observed to a minimal degree as a late response in the present study. The BRAF inhibition-mediated c-Met over-expression mainly affects the PI3K/AKT pathway and further studies are warranted to elucidate the core mechanism of ERK signal reactivation from BRAF inhibition. Following the treatment of PLX4032, the expression of HGF, the only ligand of c-Met was induced and this result suggests that the PLX4032-mediated over-expression of c-Met is caused, at least in some part, by the induction of the c-Met ligand (Figure 5). On the basis of the findings that c-Met is increased from PLX4032

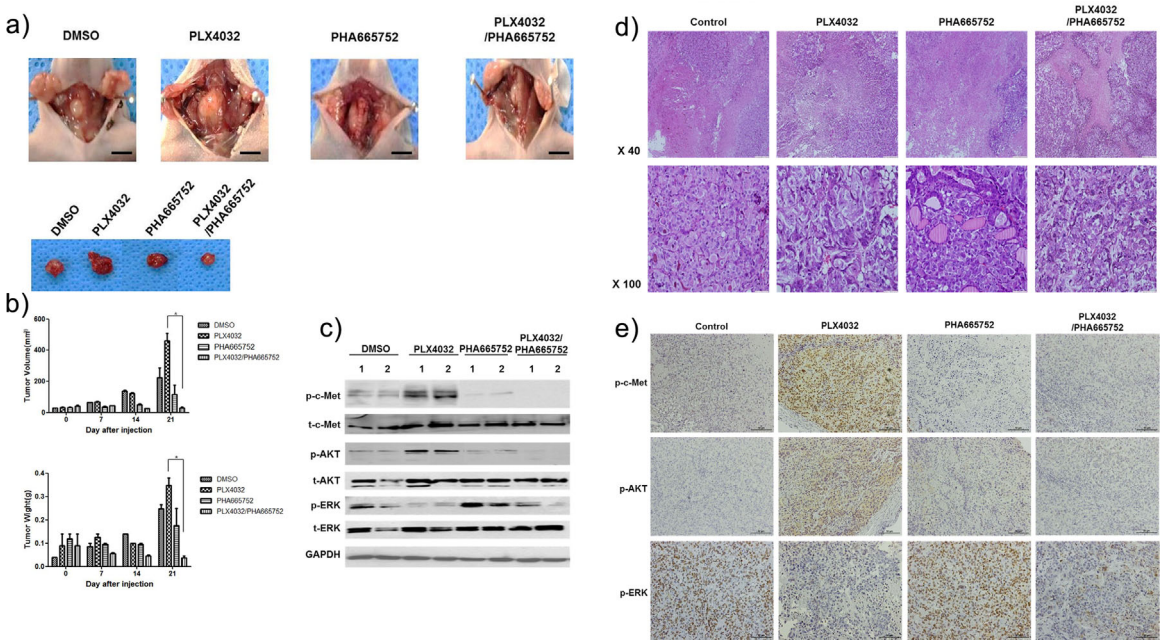

Figure 6. Treatment response to PLX4032 and PHA665752 in a xenograft mouse model orthotopically injected with 8505C cells. (a) 8505C cells were orthotopically injected in thyroid glands of BALB/c nude mice and randomly divided into four groups with different treatment conditions as follows; DMSO (20 mg/kg/day), PLX4032 (20 mg/kg/day), PHA665752 (10 mg/kg/day), and combinatorial PLX4032 (20 mg/kg/day) and PHA665752 (10 mg/kg/day) treatment. The tumor size was slightly larger or similar in the single agent treatment group when compared to control group, however, it was significantly smaller in the combinatorial treatment group. (b) Assessment of tumor volume and weight 3 wk following different drug treatments. Both tumor size and volume were larger in PLX4032 single agent treatment group when compared to control group, however the values were significantly smaller in the combinatorial treatment group. ($^*P < 0.05$) (c) Western blot analysis of intratumoral protein expression after drug treatment in tumor specimens. Both p-c-Met and p-AKT expression levels were increased in PLX4032 single treatment group, however, they were considerably decreased in combinatorial drug treatment group. (d) Histopathological analysis confirmed by H & E staining from tumor tissue samples derived from mice of each group. On $\times 40$ magnification, the tumors of drug-treatment group generally presented tumor capsule formation with pushing margins as supposed to irregular infiltrative tumor growth in the control group. Specifically, the PLX4032 single treatment group showed further aggressive features such as frequent extracapsular extension with presence of lymphovascular invasion and perineural invasion. The combinatorial drug treatment group however presented no tumor capsule invasion with lymphocytes aggregating around the tumor. Lymphovascular invasion and perineural invasion were not found. On $\times 100$ magnification, cellular degenerative change and degree of decreased cell viability was most prominent in the combinatorial treatment group. (e) Immunohistochemistry evaluation of tumor tissues from each treatment group. Compared to the control group, p-c-Met, and p-AKT detection levels were high in the PLX4032 single treatment group. In the combinatorial PLX4032 and PHA665752 treatment group, detection levels of p-c-Met, p-AKT, and p-ERK were all markedly low.

treatment in 8505C cells, combinatorial treatment of BRAF inhibitor (PLX4032) and c-Met inhibitor (PHA665752) resulted in effective suppression of both p-AKT and p-ERK, suggesting enhanced therapeutic efficacy (Figure 4). Furthermore, the results of the in vitro study were confirmed in in vivo animal experiments (Figure 6). The combinatorial treatment response of the in vivo study appears more prominent than the in vitro study which suggests the possibility of additional mechanisms such as the increased expression of HER3 [22] as previously reported and this will require further attention in the near future.

In summary, this study demonstrates that different treatment responses of BRAF inhibition are shown in different types of thyroid cancer harboring BRAF (V600E) mutation. Particularly in 8505C cells which presented decreased responses of cellular growth inhibition and tumor suppression, there exists an acquired resistance mechanism to BRAF inhibition, mediated by the increased expression of c-Met. Therefore, in BRAF (V600E) mutant anaplastic thyroid cancer which is resistant to PLX4032, the combinatorial treatment of BRAF inhibitor and c-Met inhibitor can overcome the limitation of single agent therapy and maximize the specific anti-tumor effect of targeted therapy. Whatsmore, its clinical implications are expected to be greatly extended, forming the basis of optimal personalized combinatorial targeted therapy.

ACKNOWLEDGMENTS

This work was supported by the National Research Foundation of Korea (NRF) grant funded by the Korea government (2010-0012412) and the Yonsei University College of Medicine Research Fund grant no.6-2014-0052.

REFERENCES

1. National Cancer Institute. SEER Stat Fact Sheet: Thyroid Cancer. Available at: http://seer.cancer.gov/statfacts/html/thyro.html. Accessed October 28, 2013.
2. Thyroid Cancer page. National Cancer Institute, Web site. Available at: http://www.cancer.gov/cancertopics/types/thyroid. Accessed January 18, 2010.
3. Lal G, O'Dorisio T, McDougall R, Weigel RJ. Cancer of the endocrine system In: Abeloff MD, Armitage JO, Niedernuber JE, Kastan MB, McKenna WG, editors. Abeloff's clinical oncology. 4th ed. Philadelphia, PA: Churchill Livingston; 2008. chap 75.
4. Prinz RA, Chen E. Thyroid Cancer In: Bope ET, Rakel RE, Kellerman RD, editors. Conn's current therapy 2010. Maryland Heights, MO: W. B. Saunders, Elsevier; 2009.
5. Rosove MH, Peddi PF, Glaspy JA. BRAF V600E inhibition in anaplastic thyroid cancer. N Engl J Med 2013;368:684–685.
6. Witt RL, Ferris RL, Pribitkin EA, Sherman SI, Steward DL, Nikiforov YE. Diagnosis and management of differentiated thyroid cancer using molecular biology. Laryngoscope 2013;123:1059–1064.
7. Nikiforova MN, Kimura ET, Gandhi M, et al. BRAF mutations in thyroid tumors are restricted to papillary carcinomas and anaplastic or poorly differentiated carcinomas arising from papillary carcinomas. J Clin Endocrinol Metab 2003;88:5399–5404.
8. Takano T, Ito Y, Hirokawa M, Yoshida H, Miyauchi A. BRAF V600E mutation in anaplastic thyroid carcinomas and their accompanying differentiated carcinomas. Br J Cancer 2007;96:1549–1553.
9. Hall RD, Kudchadkar RR. BRAF mutations: Signaling, epidemiology, and clinical experience in multiple malignancies. Cancer Control 2014;21:221–230.
10. Chapman PB, Hauschild A, Robert C, et al. Improved survival with vemurafenib in melanoma with BRAF V600E mutation. N Engl J Med 2011;364:2507–2516.
11. Dietrich S, Glimm H, Andrulis M, von Kalle C, Ho AD, Zenz T. BRAF inhibition in refractory hairy-cell leukemia. N Engl J Med 2012;366:2038–2040.
12. Kopetz S, Desai J, Chan E, et al. PLX4032 in metastatic colorectal cancer patients with mutant BRAF tumors. J Clin Oncol 2010;28:15s.
13. Hayes DN, Lucas AS, Tanvetyanon T, et al. Phase II efficacy and pharmacogenomic study of Selumetinib (AZD6244; ARRY-142886) in iodine-131 refractory papillary thyroid carcinoma with or without follicular elements. Clin Cancer Res 2012;18:2056–2065.
14. Girotti MR, Marais R. Deja Vu: EGF receptors drive resistance to BRAF inhibitors. Cancer Discov 2013;3:487–490.
15. Cohen Y, Rosenbaum E, Clark DP, et al. Mutational analysis of BRAF in fine needle aspiration biopsies of the thyroid: A potential application for the preoperative assessment of thyroid nodules. Clin Cancer Res 2004;10:2761–2765.
16. Kimura ET, Nikiforova MN, Zhu Z, et al. High prevalence of BRAF mutations in thyroid cancer: Genetic evidence for constitutive activation of the RET/PTC-RAS-BRAF signaling pathway in papillary thyroid carcinoma. Cancer Res 2003;63:1454–1457.
17. Xing M, Tufano RP, Tufaro AP, et al. Detection of BRAF mutation on fine needle aspiration biopsy specimens: A new diagnostic tool for papillary thyroid cancer. J Clin Endocrinol Metab 2004;89:2867–2872.
18. Xing M. BRAF mutation in thyroid cancer. Endocr Relat Cancer 2005;12:245–262.
19. Lee J, Hwang JA, Lee EK. Recent progress of genome study for anaplastic thyroid cancer. Genomics Inform 2013;11:68–75.
20. Corcoran RB, Ebi H, Turke AB, et al. EGFR-mediated reactivation of MAPK signaling contributes to insensitivity of BRAF mutant colorectal cancers to RAF inhibition with vemurafenib. Cancer Discov 2012;2:227–235.
21. Straussman R, Morikawa T, Shee K, et al. Tumour microenvironment elicits innate resistance to RAF inhibitors through HGF secretion. Nature 2012;487:500–504.
22. Montero-Conde C, Ruiz-Llorente S, Dominguez JM, et al. Relief of feedback inhibition of HER3 transcription by RAF and MEK inhibitors attenuates their antitumor effects in BRAF-mutant thyroid carcinomas. Cancer Discov 2013;3:520–533.